Journal of Molecular Liquids 229 (2017) 45–50

Contents lists available at ScienceDirect

Journal of Molecular Liquids

journal homepage: www.elsevier.com/locate/molliq

Formation and characterization of microcantilevers produced from ionic liquid by electron beam irradiation

Triinu Taaber [a,b], Mikk Antsov [a,*], Sergei Vlassov [a], Uno Mäeorg [b], Leonid Dorogin [c], Martin Järvekülg [a], Kristjan Saal [a], Rünno Lõhmus [a]

[a] Institute of Physics, University of Tartu, W. Ostwaldi Str. 1., 50411 Tartu, Estonia
[b] Institute of Chemistry, University of Tartu, Ravila 14A, 50411 Tartu, Estonia
[c] Peter Grünberg Institute and Institute for Advanced Simulation, Forschungszentrum Jülich GmbH, Wilhelm-Johnen-Straße, 52428 Jülich, Germany

ARTICLE INFO

Article history:
Received 4 August 2016
Received in revised form 14 November 2016
Accepted 9 December 2016
Available online 16 December 2016

Keywords:
Polymers
Mechanical properties
Solidification
Electron microscopy
Lithography

ABSTRACT

Recently, ionic liquids (ILs) have been recognized to have significant potential as precursors or reaction media in nanolithography and MEMS component technologies. In this work, we demonstrate straightforward fabrication of positioned and well-defined microscale structures by electron beam (e-beam) irradiation of two different ILs: 1-hexyl-3-methylimidazolium bis(trifluoromethylsulfonyl)imide (HMIM TFSI) and 1-(6-hydroxyhexyl)-3-methylimidazolium bis(trifluoromethylsulfonyl)imide (HMIM-OH TFSI). The study includes comparison between the compositions and mechanical properties of corresponding e-beam-irradiated ILs. The average Young's moduli of prepared IL microcantilevers measured in beam bending tests were found to be 7.2 ± 0.9 GPa and 3.5 ± 1.3 GPa for HMIM-OH TFSI and HMIM TFSI, respectively. Infrared spectroscopy indicated the formation of polymer in e-beam-irradiated HMIM-OH TFSI, while structures from HMIM TFSI melted in ambient conditions. The presented results showcase the potential IL precursors in microscopic 3-D printing approaches for mechanical elements in MEMS technologies as well as for developing reversibly solidified precursors for lithography.

1. Introduction

Room temperature ionic liquids (RTIL) have been extensively studied [1,2] and have been demonstrated to have great potential in various applications [3,4] because of their unique combination of electrical [5], thermal [6], chemical [7], tribological [8] and other properties. Due to their characteristic low vapor pressure, RTIL can be used in high-vacuum conditions and studied by scanning electron microscopy (SEM) [9]. As recognized and demonstrated in earlier works, such combination of features can suggest vacuum technologies with new and exciting possibilities. In addition to functions in material characterization methods [10], ILs can serve as a medium for localized synthesis of various structures by electron beam (e-beam) irradiation. Schmuki et al. demonstrated the formation of Ag nanodendrites on anatase TiO_2 surface in 1-butyl-3-methylimidazlium tetrafluoroborate [BMIM][BF4] under exposure to e-beam in a high-vacuum SEM chamber [11]. Imanishi et al. have reported e-beam-promoted synthesis of Au nanoparticles in an IL via a reductive reaction [12] and pointed to the method's potential application in nanolithography, if those particles could be attached to the surface.

In addition to serving as a functional reaction medium, ILs themselves can undergo polymerization. Polymerized ILs have been found to have many interesting properties suitable for a range of applications including polymeric electrolytes [13], microwave-absorbers [14], ionic conductors [15], and porous materials [16]. Pre-polymerized forms of ILs have been used as a nonvolatile conductive component in producing composites [17]. Among other strategies, polymerization of ILs can be driven by exposure to radiation. Ionizing radiation (e.g. e-beam) interacts with matter and yields reactive species such as radical ions and solvated electrons [18]. These reactive species may initiate several fragmentations, modifications and chemical reactions, including IL polymerization.

Recently, polymerizable RTILs precursors have also been applied to micro- and nanoscale lithography to produce positioned patterns on substrates. Bocharova et al. [19] reported direct writing in IL by strong electric fields localized by the tip of an atomic force microscope (AFM). E-beam-induced polymerization of up to 1 μm thick 1-allyl-3-ethylimidazolium bis(trifluoromethylsulfonyl)imide [AllylEtIm][TFSI] layers was demonstrated by Minamimoto et al. [20]. By the latter method, various three-dimensional structures were produced on Si substrate with sub-100 nm resolution. However, the applicability of 3D printing in RTIL should not be limited to on-substrate lithography. The availability of different ionizing radiations at different energies and the wide

* Corresponding author.
E-mail address: mikk.antsov@ut.ee (M. Antsov).

http://dx.doi.org/10.1016/j.molliq.2016.12.034
0167-7322/

range of ions that can be combined in RTILs with suitable susceptibility suggest that direct writing of suspended and cantilevered domains of polymerized IL is also possible.

In this paper, e-beam-induced polymerization was applied to RTILs 1-hexyl-3-methylimidazolium bis(trifluoromethylsulfonyl)imide (HMIM TFSI) and 1-(6-hydroxyhexyl)-3-methylimidazolium bis (trifluoromethylsulfonyl)imide (HMIM-OH TFSI) to produce free-standing microcantilevers (MC) attached to a silicon AFM tip. Observations were made on the geometry of formed structures, and IR spectroscopy was used to monitor differences in the changes that occur in similar ILs. A real-time nanomanipulation technique inside an SEM [21–24] was applied to determine the mechanical properties of the obtained ionic liquid microcantilevers (ILMC) in situ in order to demonstrate the potential of the applied approach in direct bottom-up 3D writing of mechanical elements for MEMS and to explore the influence of hydroxyl group IL on the behavior and properties of the ILMCs.

2. Experimental

2.1. Materials

N-methylimidazole (Aldrich), lithium bis(trifluoromethanesulfonyl) imide (Merck), dichloromethane (Lachner), HMIM TFSI (Merck) and all solvents were used as received. α,ω-Bromoalcohols were synthesized from the corresponding α,ω-diols (Aldrich) using a standard procedure [25]. HMIM-OH TFSI was prepared by treating *N*-methylimidazole (0.1 mol) with 6-bromoalcohol (0.1 mol) at room temperature under inert atmosphere for 24–48 h as reported previously [26]. 1-(6-Hydroxyhexyl)-3-methylimidazolium bis(trifluoromethylsulfonyl) imide (HMIM-OH TFSI) was prepared through an anion exchange with 1-(6-hydroxyhexyl)-3-metylimidazolium bromide using a standard protocol [27].

2.2. Formation of the ionic liquid microcantilevers

Neat ILs were drop-casted onto untreated silicon wafer (oxidized, Semiconductor Wafer Inc.) and placed inside the vacuum chamber of the SEM (TESCAN Vega-II SBU) equipped with 3D-nanomanipulator (Smaract) with attached silicon AFM cantilever (ATEC-CONT cantilevers, Nanosensors, C = 0.2 N m^{-1}, tip radius approx. 20 nm). The geometry of the AFM cantilever enabled tip visibility from the top.

Prior formation of the microstructure from the IL, the AFM tip was immersed and held in the IL droplet (Fig. 1(a)). SEM imaging at this stage was performed under low current density (≪1 A m^{-2}) to avoid unintentional structural changes in the IL. Then, the rectangular area adjacent to the AFM tip was chosen and locally irradiated with e-beam of the much higher current density (on the order of 1 A m^{-2}) to cause a local solidification of the IL. Rapid change in contrast in the irradiated area served as an indication of the solidification onset: irradiated areas appeared darker in the SEM image. The polymerization/solidification process was saturated as soon as no further changes in contrast were observed. This process resulted in the formation of a solid rectangular structure on top of the IL droplet surface, attached to the AFM tip from one end. After the solidification, the probing current was decreased to avoid further solidification of the surrounding IL. The tip was then retracted from the IL, exposing the free-standing beam as seen in Fig. 1(b).

2.3. Geometrical and mechanical characterization

Thickness and uniformity of the geometry of ILMCs were measured in SEM in a series of manipulations in which polymerized/solidified ILMC was rotated and tilted at different angles in order to observe it from different points of view.

Young's moduli of the ILMCs were measured in a bending test performed by pushing the free end of the ILMC against the end of the fixed reference AFM cantilever with known stiffness (Fig. 2). The deformation of the reference AFM cantilever enabled the calculation of the force acting on the bent ILMC. The elastic beam theory was applied to fit the experimentally obtained SEM image of the bent ILMC. A flexible beam of length L with Young's modulus E and area moment of inertia I with point load f at its end over axis l of the beam has an equilibrium bending profile governed by the differential equation:

$$EI\theta''(l) + f\cos[\theta(l)] = 0, \tag{1}$$

and is subject to the following boundary conditions: $\theta(0) = 0$ and $\theta'(L) = 0$, where $\theta(l)$ is the tangential bending angle with respect to the initial straight profile [28]. The area moment of inertia for a beam with rectangular cross-section is expressed as $I = bh^3/12$, where b is the width and h is the thickness of the beam. As a result of the fitting, the Young's modulus for each ILMC was determined.

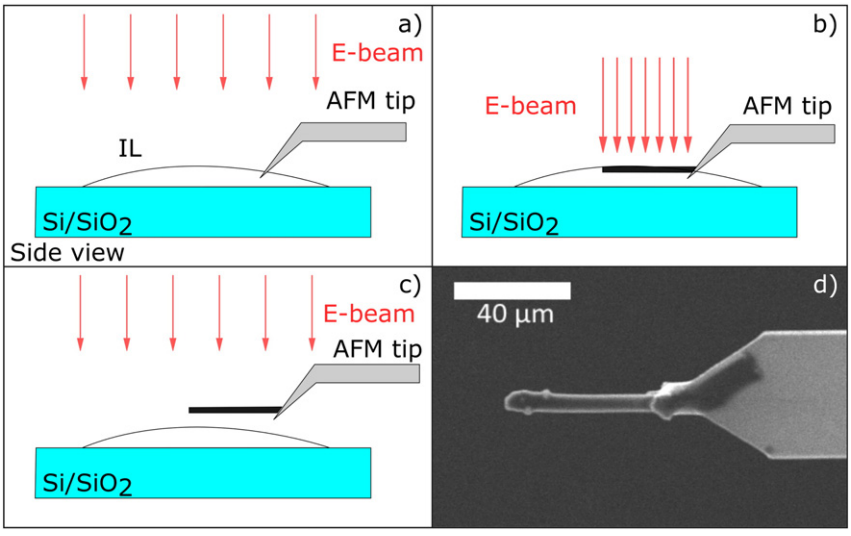

Fig. 1. Schematics of the ILMC formation inside SEM: a) AFM tip submerged in IL under the low current density, b) rectangular area adjacent to AFM tip is irradiated with high current density e-beam causing local polymerization/solidification of the IL, c) free-standing ILMC is exposed by lifting AFM tip, d) experimental image of the ILMC attached to the AFM cantilever.

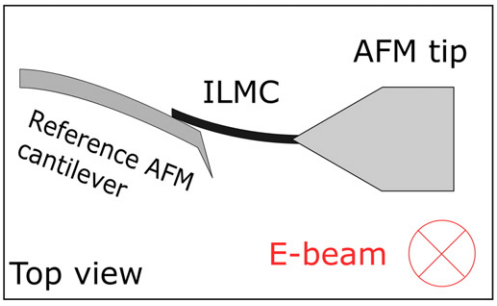

Fig. 2. Schematic of the bending test: ILMC is bent against a reference AFM cantilever with known stiffness.

2.4. Chemical characterization

Chemical compositions of the ILs HMIM-OH TFSI and HMIM TFSI and respective e-beam-irradiated ILs were investigated with an FTIR Bruker Vertex 70 Spectrum Fourier transform infrared spectroscopy (FT-IR) instrument. For sample preparation, approximately 1 mm^2 IL on silicon wafer was irradiated with e-beam and subsequently washed with methanol to remove unaffected IL.

3. Results and discussion

Dependence of the ILMC formation dynamics on current density, exposure time and energy of electrons was investigated. The main attribute that was used as an indication of IL polymerization/solidification onset was rapid and irreversible change in contrast (darkening) in the irradiated area relative to the surrounding IL. As was later confirmed, polymerization/solidification was saturated when no further change in contrast at the given e-beam parameters was observed. It was shown that from this point further irradiation had no additional effect on the thickness and apparent properties of the formed structure. It was found that for 10 kV accelerating voltage, steady continuous polymerization/solidification starts at threshold current density on the order of 1 A m^{-2}. The rate of complete polymerization/solidification increased from approximately 15 s to a few seconds with increasing current density from 1 A m^{-2} to 2.5 A m^{-2}. For higher current densities, controllable formation of the ILMC became more problematic due to drift of the IL pattern caused by excessive charging and formation of the bubbles starting from 4.7 A m^{-2}. Observed outgassing could be due to the radiation-induced decomposition of the IL in the irradiated area. Shkrob et al. [29] have demonstrated the decomposition of IL by 3 MeV electron radiation by analyzing the radical composition of the fragmented IL by electron paramagnetic resonance and mass spectroscopy. Various radicals formed upon the e-beam radiation and can induce different chemical reactions that can yield gaseous (e.g. hydrogen) or higher vapor pressure products. Another explanation for the formation of bubbles could be the presence of small impurities in the form of nanoparticles, which act as catalysts in e-beam- or current-induced electro-chemical reactions [30]. These nanoparticles may be smaller than the resolution of the SEM or just may not be visible in the IL medium [31].

3.1. Effect on ILMC thickness

In order to investigate the effect of prolonged e-beam irradiation times on ILMC thickness, a series of measurements were collected at 10 keV and 2.5 A m^{-2} with irradiation times ranging from 5 s (corresponding to saturation of the contrast change) to 60 s. It was found that prolonged exposure to high current density electrons had negligible effect on ILMC thickness (Fig. 3(a). The average thickness of the ILMC obtained at different irradiation times was 1.3 ± 0.2 μm. The dependence of the irradiated ILMC thickness on electron energy was

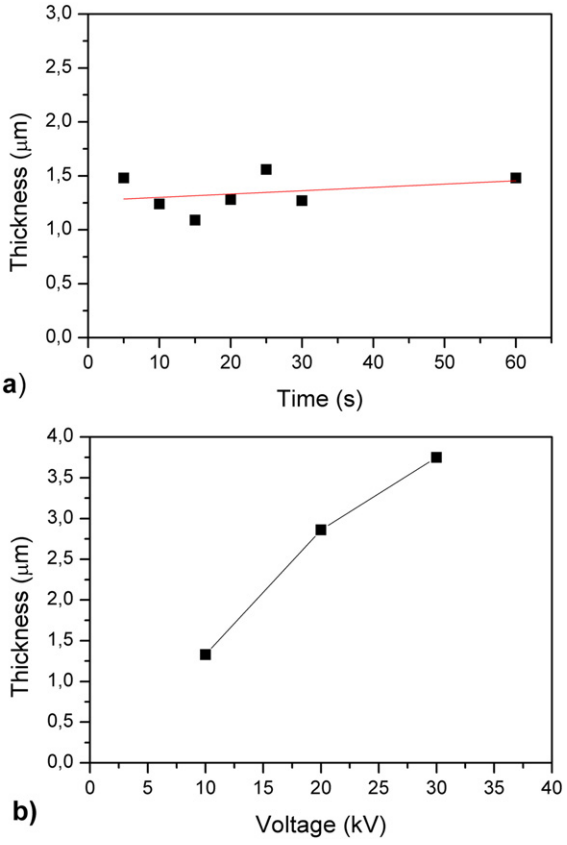

Fig. 3. HMIM-OH TFSI MC thickness as a function of (a) exposure time at 10 kV electron beam accelerating voltage and (b) the electron beam accelerating voltage at 15 s of exposure. The current density was 2.5 A m^{-2}.

investigated for three accelerating voltages: 10, 20 and 30 kV. As was expected, results revealed strong dependence of the thickness on the accelerating voltage in the studied energy region (Fig. 3(b). This can be easily explained, as electron penetration depth in liquid is determined by their energy. The penetration depth d of an incident e-beam in different materials can be roughly estimated as [32]:

$$d = 0.1 * \frac{{E_0}^{1.5}}{\rho}, \quad (2)$$

where E_0 is the accelerating voltage in keV, ρ is the density of the penetrated material, and d reads in μm. HMIM TFSI was therefore expected to act similarly to HMIM-OH TFSI because of having approximately the same density (1.37 g cm^{-3} as was estimated from literature [33] considerations). Eq. (2) for the accelerating voltage of 10 keV and liquid density of 1.37 g cm^{-3} yields a penetration depth on the order of 2 μm, which is in the same range as the experimentally measured thickness of the ILMCs. For reference, in a pure water environment, the penetration depth of electrons with 10 keV energy was estimated to have an average value of 1.31 μm [34].

For all studied current densities, structures obtained with variety of irradiation times and voltages had well-defined edges and rectangular cross-sections, as was revealed in a series of manipulations in which solidified ILMC was attached to the AFM tip by unmodified IL, enabling easy rotation and tilting of the ILMC by pushing it against the hard Si substrate (Fig. 4).

3.2. Young's modulus measurements

Young's modulus measurements were performed on 9 HMIM-OH TFSI and 13 HMIM TFSI MCs, with the average length of the suspended

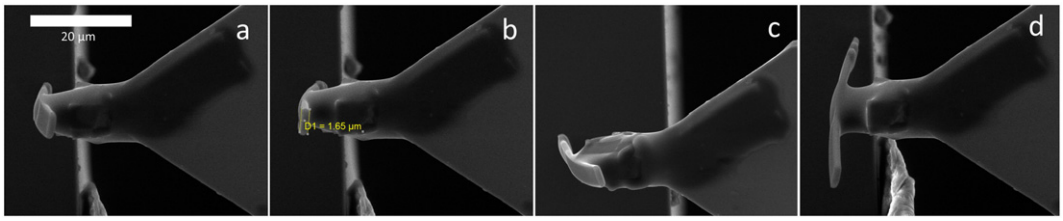

Fig. 4. Series of manipulations of the ILMC on top of a hard Si substrate with the purpose to observe its geometry from different angles.

portion of 40 µm and average width of 4 µm. The measured average Young's moduli were 7.2 ± 0.9 GPa and 3.5 ± 1.3 GPa for HMIM-OH TFSI and HMIM TFSI, respectively. These values are in the same range as the Young's moduli of different well-known polymers [35].

Neither bending strength nor the joint strength between ILMC and Si tip was measured since sliding along the reference cantilever appeared earlier than possible fracture. However, it can be concluded that ILMC can be reversibly bent to high curvatures (Fig. 5) multiple times without any noticeable signs of fracture, and bending strength should exceed 12.6 GPa, which is the maximal bending stress registered before sliding. This demonstrates that ILMC can serve as an elastic durable cantilever and that strong binding to Si can be achieved without any surface modification. Thus, the studied RTIL shows excellent compatibility with conventional silicon-based lithography and MEMS technologies.

3.3. IR analysis

In the next step, IR spectroscopy of polymerized ILs was performed to gain insight into the processes that occur in ILs during e-beam exposure. For IR studies, larger areas were irradiated to enable mechanical transfer of the obtained structure for spectroscopic analysis. For HMIM-OH TFSI, the processed IL had formed a solid film and could be easily detached from the Si wafer. Irradiated HMIM TFSI, however, turned into a soft gel-like material at ambient conditions that made mechanical transfer difficult and was measured on the Si wafer. The IR spectra of HMIM-OH TFSI before and after irradiation with e-beam are shown in Fig. 6(a) and (b), respectively. In the spectrum of HMIM-OH TFSI (Fig. 6(a), the —OH band appeared at 3555 cm^{-1} and 3398 cm^{-1}. Multiple peaks around 3100 cm^{-1} were derived from the C—H stretching of the imidazolium cation. The signals at 2939 cm^{-1} and 2865 cm^{-1} were attributed to the C—H bond stretching of the imidazolium side chain, and 1463 cm^{-1} was assigned to the C^{+}═N— bond of the imidazolium cation [36]. The absorption bands around 1400–1000 cm^{-1} were assigned to the TFSI anion [37].

After the irradiation of HMIM-OH TFSI with the e-beam, the IR spectrum changed (Fig. 6(b). Firstly, the small peaks at 3555 cm^{-1} and 3398 cm^{-1} arising from the —OH group disappeared, which may indicate that the hydroxyl group had been eliminated and that an aromatic ring had formed [38]. The IR spectrum of the electron beam-irradiated HMIM-OH TFSI is very similar to the spectrum of polymers with aromatic group, i.e. polystyrene [39]. In Fig. 6(b), the absorbance bands around 1400–1000 cm^{-1} of the TFSI anion are still visible, but the intensities are significantly lower. This may be due to the attack of an anion to the methyl group of the imidazolium cation [37]. Small peaks at 2000–1700 cm^{-1} can be seen, which together with 752 cm^{-1} and 695 cm^{-1} indicates the monosubstituted aromatic ring. It may be suggested that polymer was obtained due to the recombination of cations that are transformed into radicals. The addition of hydroxyl group would be beneficial for this process, as it will direct the deprotonation from methylene. Although the exact details of polymerization in this case will have to be addressed in future studies, it is noteworthy that underlying mechanisms have to be essentially different from double-bond-enabled reactions in prior RTIL polymerization cases [13,14].

The IR spectrum of electron-irradiated HMIM TFSI has less-pronounced changes. In the spectrum of HMIM TFSI shown in Fig. 7(a), multiple signals around 3100 cm^{-1} are attributed to the C—H stretching of the imidazolium cation. The peaks at 2939 and 2860 cm^{-1} are from the C—H bond stretching of the imidazolium side chain, and 1463 cm^{-1} was assigned to the C^{+}═N— bond of the imidazolium cation. The absorption bands of the TFSI anion are observed around 1400–1000 cm^{-1}. In the IR spectrum of electron-irradiated HMIM TFSI shown in Fig. 7(b), a new absorption band at 1655 cm^{-1} is the only significant change. This signal may indicate the presence of alkyl amine. Since the decomposition of ILs is generally caused by the nucleophilic anion attack to the cation and the TFSI anion is a weak nucleophile, it decomposes to a more nucleophilic atom or group [40]. More nucleophilic groups F and NH_2 may attack the methyl or hexyl chain of the cation, and an alkyl amine is generated. The real mechanism of e-beam irradiation on HMIM TFSI needs to be further studied.

IR spectra correlate well with measured mechanical properties of irradiated materials. Higher elastic modulus (7.2 GPa) of MCs from HMIM-OH TFSI as well as the fact that intact films could be peeled off in the experiments support the hypothesized polymerization and formation of polymer with aromatic group, i.e. polystyrene. The mechanical properties of the obtained polymerized IL and corresponding cantilevers can be expected to be independent of the surrounding environment. Lower elastic modulus of cantilevers from HMIM TFSI (3.5 GPa) and a spontaneous change that can be described as melting in ambient environment are in agreement with less or no intermolecular bonding caused by e-beam exposure that was indicated by FTIR. While this kind of performance can be initially interpreted as proof of

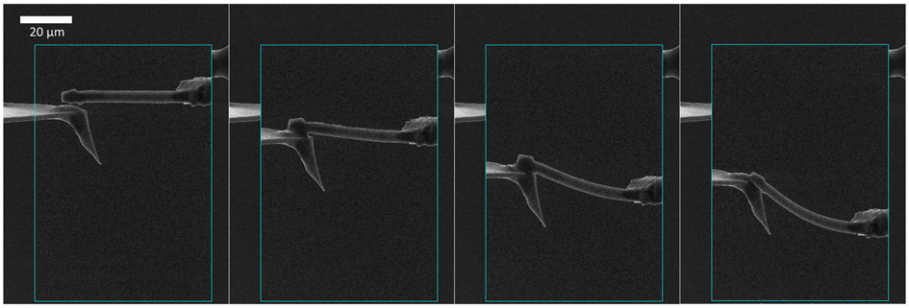

Fig. 5. Bending test of HMIM-OH TFSI MC.

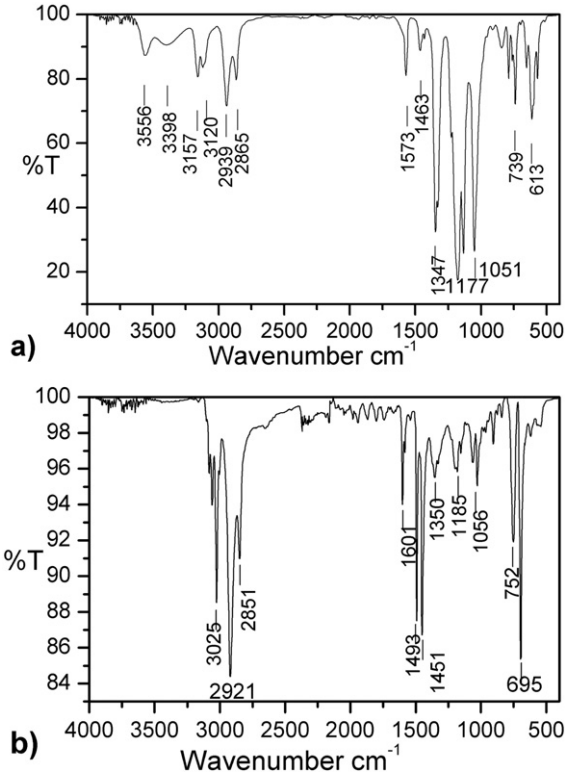

Fig. 6. The IR spectra of HMIM-OH TFSI (a) before and (b) after irradiation with e-beam.

inferior mechanical stability, the feature of reversible solidification by e-beam can open up new perspectives in lithography, e.g. spontaneously removable masks or temporary adhesives. Although the real mechanism of the influence of the electron beam irradiation on HMIM TFSI and HMIM-OH TFSI requires additional investigation, direct 3D writing of well-defined, positioned and attached microscale elements can be performed in both of these similarly composed and structured RTILs in a straightforward manner.

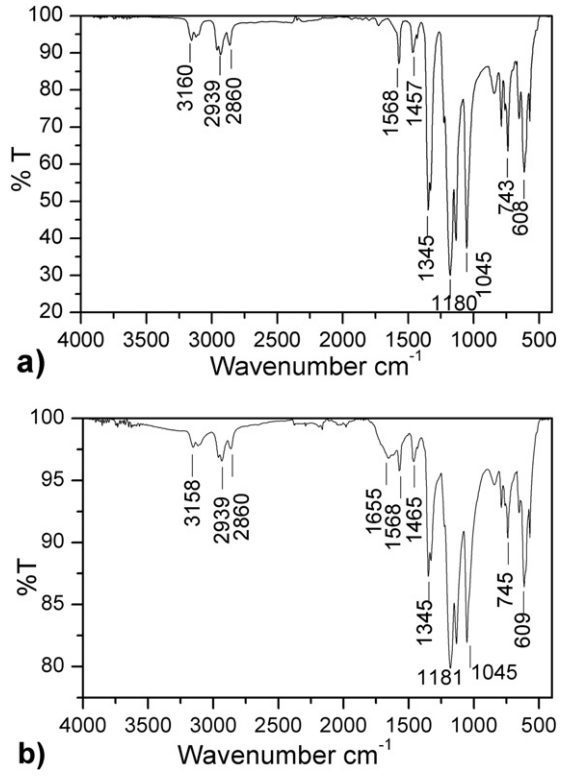

Fig. 7. The IR spectra of HMIM TFSI (a) before and (b) after irradiation with e-beam.

4. Conclusions

In this work, a novel method for fabricating ionic liquid microcantilevers (ILMC) from HMIM TFSI and HMIM-OH TFSI ILs by localized irradiation with electron beam was demonstrated. Dependence of the formation dynamics of the ILMC on current density, exposure time and accelerating voltage was determined. It was found that steady and stable formation of ILMC was possible at current densities between 1 A m^{-2} and 4.7 A m^{-2}. Complete solidification was achieved on the order of a few seconds, and further irradiation had no effect on ILMC thickness. On the other hand, thickness directly depended on the accelerating voltage ranging from 1.3 to 3.75 μm for voltage in the range of 10 to 30 kV at current density of 2.5 A m^{-2}. In situ SEM cantilever beam bending technique was applied for mechanical characterization of the ILMC. The Young's moduli of HMIM TFSI and HMIM-OH TFSI were 3.5 ± 1.3 GPa and 7.2 ± 0.9 GPa, respectively, which is indicative of typical polymeric materials. It was demonstrated that ILMCs can withstand relatively high mechanical stresses (at least 12.6 GPa) without fracture and are strongly bonded to the Si tip, which makes them good candidates for applications as durable and flexible cantilevers in Si-based MEMS technologies. In addition, it was shown that the hydroxyl group of IL has an important role in the polymerization/solidification process and affects the mechanical properties. The described method enables new applications of in situ SEM fabrication, manipulation and attachment of structural components.

Acknowledgements

This work was supported by the Estonian Science Foundation (grants JD162, IUT2-25), and European Union through the European Regional Development Fund (Centre of Excellence "Advanced materials and high-technology devices for sustainable energetics, sensorics and nanoelectronics", TK141). The work was also partly supported by COST Action MP1303. L.D. was partly supported by the International Research Laboratory Initiative of ITMO University.

References

[1] T. Torimoto, T. Tsuda, K. Okazaki, S. Kuwawata, New frontiers in materials science opened by ionic liquids, Adv. Mater. 22 (2010) 1196–1221.
[2] I. Minami, Ionic liquids in tribology, Molecules 14 (2009) 2262–2269.
[3] J.L. Bideau, L. Vidau, A. Vioux, Ionogels, ionic liquid based hybrid materials, Chem. Soc. Rev. 40 (2011) 907–925.
[4] A.E. Jimenez, M.D. Bermudez, F.J. Carrion, G. Martinez-Nicolas, Room temperature ionic liquids as lubricant additives in steel–aluminium contacts: influence of sliding velocity, normal load and temperature, Wear 261 (2006) 347–359.
[5] P. Hapiot, C. Lagrost, Electrochemical reactivity in room-temperature ionic liquids, Chem. Rev. 108 (7) (2008) 2238–2264.
[6] P.S. Wheatley, P.K. Allan, S.J. Teat, S. Ashbrook, R.E. Morris, Task specific ionic liquids for the ionothermal synthesis of siliceous zeolites, Chem. Sci. 1 (2010) 483–487.
[7] T. Welton, Ionic liquids in catalysis, Coord. Chem. Rev. 248 (21–24) (2004) 2459–2477.
[8] Y. Han, D. Qiao, L. Zhang, D. Feng, Study of tribological performance and mechanism of phosphonate ionic liquids for steel/aluminum contact, Tribol. Int. 84 (2015) 71–80.
[9] S. Kuwabata, A. Kongkanand, D. Oyamatsu, T. Torimoto, Observation of ionic liquid by scanning electron microsocope, Chem. Lett. 35 (6) (2006) 600–601.
[10] T. Tsuda, N. Nemoto, K. Kawakami, E. Mochizuki, S. Kishida, T. Tajiri, T. Kushibiki, S. Kuwabata, SEM observation of wet biological specimens pretreated with room-temperature ionic liquid, Chem. Biol. Chem. 12 (17) (2011) 2547–2550.
[11] P. Roy, R. Lynch, P. Schmuki, Electron beam induced in-vacuo Ag deposition on TiO2 from ionic liquids, Electrochem. Commun. 11 (8) (2009) 1567–1570.
[12] A. Imanishi, M. Tamura, S. Kuwabata, Formation of Au nanoparticles in an ionic liquid by electron beam irradiation, Chem. Commun. 13 (2009) 1775–1777.
[13] T. Sato, S. Marukane, T. Narutomi, T. Akao, High rate performance of a lithium polymer battery using a novel ionic liquid polymer composite, J. Power Sources 164 (1) (2007) 390–396.

[14] S. Amajjahe, H. Ritter, Microwave-sensitive foamable poly(ionic liquids) bearing tert-butyl ester groups: influence of counterions on the ester pyrolysis, Macromol. Rapid Commun. 30 (2) (2009) 94–98.
[15] N. Matsumi, K. Sugai, M. Miyake, H. Ohno, Polymerized ionic liquids via hydroboration polymerization as single ion conductive polymer electrolytes, Macromolecules 39 (20) (2006) 6924–6927.
[16] F. Yan, J. Texter, Surfactant ionic liquid-based microemulsions for polymerization, Chem. Commun. 25 (2006) 2696–2698.
[17] H. Chen, Y.A. Elabd, Polymerized ionic liquids: solution properties and electrospinning, Macromolecules 42 (9) (2009) 3368–3373.
[18] I.A. Shkrob, T.W. Marin, S.D. Chemerisov, J. Hatcher, J.F. Wishart, Toward radiation-resistant ionic liquids. Radiation stability of sulfonyl imide anions, J. Phys. Chem. B 116 (30) (2012) 9043–9055.
[19] V. Bocharova, A.L. Agapov, A. Tselev, L. Collins, R. Kumar, S. Berdzinski, V. Strehmel, A. Kisliuk, I.I. Kravchenko, B.G. Sumpter, A.P. Sokolov, S.V. Kalinin, E. Strelcov, Controlled nanopatterning of a polymerized ionic liquid in a strong electric field, Adv. Funct. Mater. 25 (5) (2015) 805–811.
[20] H. Minamimoto, H. Irie, T. Uematsu, T. Tsuda, A. Imanishi, S. Seki, S. Kuwabata, Polymerization of room-temperature ionic liquid monomers by electron beam irradiation with the aim of fabricating three-dimensional micropolymer/nanopolymer structures, Langmuir 31 (14) (2015) 4281–4289.
[21] S. Vlassov, B. Polyakov, L. Dorogin, M. Antsov, M. Mets, M. Umalas, R. Saar, R. Lõhmus, I. Kink, Elasticity and yield strength of pentagonal silver nanowires: in situ bending tests, Mater. Chem. Phys. 134 (3) (2014) 1026–1031.
[22] S. Vlassov, B. Polyakov, L. Dorogin, M. Vahtrus, M. Mets, M. Antsov, R. Saar, A. Romanov, A. Lõhmus, R. Lõhmus, Shape restoration effect in Ag-SiO_2 core-shell nanowires, Nano Lett. 14 (9) (2014) 5201–5205.
[23] B. Polyakov, M. Antsov, S. Vlassov, L. Dorogin, M. Vahtrus, R. Zabels, S. Lange, R. Lõhmus, Mechanical properties of sol–gel derived SiO_2 nanotubes, Beilstein J. Nanotechnol. 5 (2014) 1808–1814.
[24] M. Antsov, L. Dorogin, S. Vlassov, B. Polyakov, M. Vahtrus, K. Mougin, R. Lõhmus, I. Kink, Analysis of static friction and elastic forces in a nanowire bent on a flat surface: a comparative study, Tribol. Int. 72 (2014) 31–34.
[25] M. Chong, M.A. Heuft, P. Rabbat, Solvent effects on the monobromination of alpha,omega-diols: a convenient preparation of omega-bromoalkanols, J. Organomet. Chem. 65 (18) (2000) 5837–5838.
[26] K. Põhako-Esko, T. Taaber, K. Saal, R. Lõhmus, I. Kink, U. Mäeorg, New method for synthesis of methacrylate-type polymerizable ionic liquids, Synth. Commun. 43 (21) (2013) 2846–2852.
[27] A.S. Shaplov, L. Goujon, F. Vidal, E.I. Lozinskaya, F. Meyer, I.A. Malyshkina, C. Chevrot, D. Teyssie, I.L. Odinets, Y.S. Vygoskii, Ionic IPNs as novel candidates for highly conductive solid polymer electrolytes, J. Polym. Sci., Part A: Polym. Chem. 47 (17) (2009) 4245–4266.
[28] L.M. Dorogin, S. Vlassov, B. Polyakov, M. Antsov, R. Lõhmus, I. Kink, A.E. Romanov, Real-time manipulation of ZnO nanowires on a flat surface employed for tribological measurements: experimental methods and modeling, Phys. Status Solidi B 250 (2013) 305–317.
[29] I.A. Shkrob, T.W. Marin, S.D. Chemerisov, J.L. Hatcher, J.F. Wishart, Radiation induced redox reactions and fragmentation of constituent ions in ionic liquids. 2. Imidazolium cations, J. Phys. Chem. B 115 (14) (2011) 3889–3902.
[30] P.J. Dyson, T.J. Geldbach, Metal Catalysed Reactions in Ionic Liquids, Springer Verlag GmbH & Co. KG, 2005.
[31] S. Arimoto, M. Sugimura, H. Kageyama, T. Torimoto, S. Kuwabata, Development of new techniques for scanning electron microscope observation using ionic liquid, Electrochim. Acta 53 (2008) 6228–6234.
[32] P.J. Potts, A Hand Book of Silicate Rock Analysis, Chapman and Hall, NY, 1987 336.
[33] S. Zhang, N. Sun, X. He, X. Lu, X. Zhang, Physical properties of ionic liquids: database and evaluation, J. Phys. Chem. Ref. Data 35 (4) (2006) 1475–1515.
[34] J.E. Turner, Interaction of ionizing radiation with matter, Health Phys. Radiat. Saf. J. (2005) 4–28.
[35] R.W. Warfield, F.R. Barnet, Elastic constants of bulk polymers, Macromol. Mater. Eng. 27 (1) (1972) 215–217.
[36] S.A. Katsyuba, P.J. Dyson, E.E. Vandyukova, A.V. Chernova, A. Vidiš, Molecular structure, vibrational spectra, and hydrogen bonding of the ionic liquid 1-ethyl-3-methyl-1H-imidazolium tetrafluoroborate, Helv. Chim. Acta 87 (10) (2004) 2556–2565.
[37] I. Rey, P. Johansson, J. Lindgren, J.C. Lassegues, J. Grondin, L. Servant, Spectroscopic and theoretical study of (CF3SO2) 2N-(TFSI-) and (CF3SO2) 2NH (HTFSI), J. Phys. Chem. A 102 (1998) 3249–3258.
[38] Z. Xue, Y. Zhang, X. Zhou, Y. Cao, T. Mu, Thermal stabilities and decomposition mechanism of amino- and hydroxyl-functionalized ionic liquids, Thermochim. Acta 578 (2014) 59–67.
[39] A.Y. León-Bermúdez, R. Salazar, Synthesis and characterization of the polystyrene – asphaltene graft copolymer by FT-IR spectroscopy, CT&F Ciencia. Tecnología y Futuro 3 (4) (2008) 157–167.
[40] Y. Chen, Y. Cao, Y. Shi, Z. Xue, T. Mu, Quantitative research on the vaporization and decomposition of [EMIM][Tf_2N] by thermogravimetric analysis–mass spectrometry, Ind. Eng. Chem. Res. 51 (2012) 7418–7427.